EFFECT OF IMPACTS ON CERES' SPIN EVOLUTION. Xiaochen Mao and William B. McKinnon, Department of Earth and Planetary Sciences and McDonnell Center for the Space Sciences, Washington University in St. Louis, Saint Louis, MO 63130 (mao@levee.wustl.edu)

Introduction: Ceres' cratered surface is a witness plate to its impact history. There have been many studies on collisions between asteroids to formalize effects of collisions on asteroid spins and size-frequency distributions (SFD) [1-6]. Dawn has provided exceptional high-resolution images that allow more precise cratering studies to be undertaken, and for Ceres in particular [7,8]. Holsapple and Henych [6] argue that large impacts are the key to a given asteroid's spin evolution, and we have recently proposed [9] that Ceres could have been hit by a very large impact or impacts that would have slowed it down to its present-day spin, which would help explain its degree-2 gravity and oblate shape. We have now undertaken a more detailed study of Ceres' spin evolution, to understand how likely such a spin state change might be. We designed Monte Carlo impact simulations to study Ceres' spin for a number of impacts consistent with its cratering record.

Collisions by Random Impacts: The analytical theory of impact effects on a target body is reasonably well described by previous works [1-5]. However, with the advancing computational power and capacity, it is worth revisiting these theories with a more discrete approach, instead of focusing on the average effect of multiple impacts [2-4]. Works in [6,10] have avoided the averaging approach and instead took a more discretized method to study the effect of impacts on rotation; however, their overall goals were different, with [6] focusing on the spin of all Main Belt Asteroids (MBA) and [10] on the tumbling induced by large impacts.

Therefore, to specifically address the impact history of Ceres, we have adopted the theory in the literature (e.g., [2,3]), but made necessary adjustments to fit our scope of investigation.

We start by assuming Ceres as a uniform sphere with mean radius R = 470 km [11], M_{Ceres} = 9.384 × 10^{20} kg, and rotation period P = 8.48 hr as suggested in [9] before despinning (this assumption is not important for our modeling). For any impactor colliding with Ceres, the probability of impact location is uniform over the sphere. Studies on the modeling of impacts onto Ceres [12,13], its cratering record [7], and the size SFD of main belt asteroids [14-16] constrain the total number (N = 3500) and the size range (1 km < d_{impactor} <100km) for Ceres' impactors, and the SFD

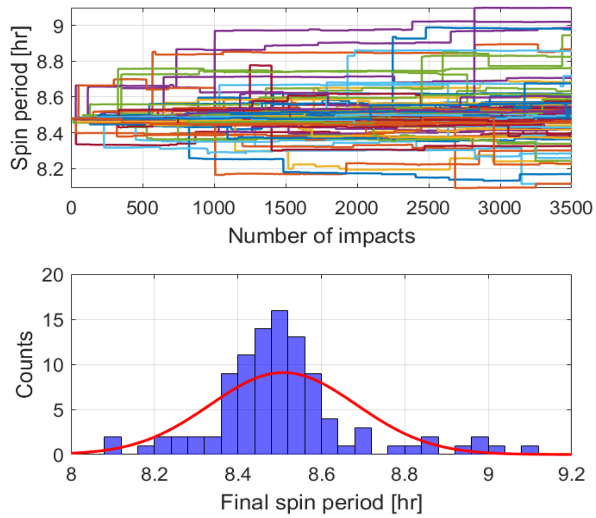

Figure 1. 100 simulations without mass loss. Each curve in the top panel is a path of spin evolution, starting at P = 8.48 hrs. Bottom panel is a histogram of the final spin period, overlain by a red Gaussian curve with mean and 1σ for the simulated results, as a comparison.

cumulative power law exponent b = 2 (less than the 2.343 in [14] from a best fit for a smaller range of asteroids, but our choice of 2 serves as a basic case). Along with a random impact angle distribution [17] and typical impact speed among asteroids (V = 5 km s^{-1}, e.g. [2]), each impactor's angular momentum at the moment of collision can be precisely quantified as $\delta\vec{\boldsymbol{L}} = m\,\vec{\boldsymbol{r}} \times \vec{\boldsymbol{V}}$, where m is the mass of a spherical impactor whose density is taken as 2000 kg m^{-3} (close to Ceres' bulk density and within the range CM chondrites [18]), $\delta\vec{\boldsymbol{L}}$, $\vec{\boldsymbol{r}}$, and $\vec{\boldsymbol{V}}$ are the angular momentum, impactor location with respect to the center of Ceres, and impact speed. Assuming angular momentum conservation and no mass loss (both assumptions are not necessarily true, as we will address later), $\delta\vec{\boldsymbol{L}} = \delta(\boldsymbol{I}\cdot\vec{\boldsymbol{\omega}}) = \delta\boldsymbol{I}\cdot\vec{\boldsymbol{\omega}} + \boldsymbol{I}\cdot\delta\vec{\boldsymbol{\omega}}$, $\delta\boldsymbol{I}$ and $\boldsymbol{I}$ are the moment of inertia added by the impactor and that of Ceres, respectively, and $\vec{\boldsymbol{\omega}}$ is the angular velocity prior to the impact (we assume $\vec{\boldsymbol{\omega}}$ is initially in the z-direction, but this is arbitrary). Thus, the change in angular velocity is

$$\delta\vec{\boldsymbol{\omega}} = \boldsymbol{I}^{-1}\cdot(m\,\vec{\boldsymbol{r}} \times \vec{\boldsymbol{V}} - \delta\boldsymbol{I}\cdot\vec{\boldsymbol{\omega}}). \qquad (1)$$

We then update Ceres' mass, radius, moment of inertia, and angular velocity after each successive impact.

Mass Loading and Escaping Ejecta: Figure 1 shows our Monte Carlo simulation results for 100 runs, with no mass loss. Each curve represents a hypothetical spin evolution path for Ceres due to random impacts. While the range of all the final spins is from 8.11 hr to 9.10 hr, 78 runs end up within 8.51 ± 0.18 hr. We also notice some extreme scenarios, involving large impacts. On the other hand, the relative flatness of most of the trajectories in Fig. 1 top panel is largely due to small impacts (large impacts with small incidence angles θ are rare). Ceres' total mass changes as impactors continue to "stick" onto it. Across these 100 simulations, the total mass of the impactors is only 0.071 ± 0.051% M_{Ceres}. This mass loading leads to a somewhat more slowly rotating Ceres on average, but the effect is trivial.

In reality, hypervelocity impact accelerates ejecta beyond the escape velocity of the target body. Thus, this part of mass loss should not simply be neglected, for there is an associated angular momentum loss as well [3]. Determining how much mass is lost requires updating scaling laws from [3]. For Ceres gravity regime scaling applies [20], and the total mass lost is given by

$$\frac{m(V_{\mathrm{ej}})}{m} = \frac{3k}{4\pi} C_1^{3\mu} \left[\frac{V_{\mathrm{ej}}}{V\cos(\theta)} \left(\frac{\rho}{\rho_{\mathrm{imp}}} \right)^{\frac{3\nu-1}{3\mu}} \right]^{-3\mu} . \quad (2)$$

In Eq. (2), $m(V_{\mathrm{ej}})$ is the ejecta mass with velocity greater than V_{ej}, C_1, k, μ are constants for a given target, $\nu = 0.4$ [20], ρ and ρ_{imp} are target and impactor density, and ρ/ρ_{imp} is taken as unity. We then followed the approach in [3] up until the averaging step, numerically integrated the change of angular velocity in the z-direction (Eq. 17 in [3] but with Eq. (2) for the ejecta mass distribution), and ran simulations with an updated Eq. (1) with the extra $-\delta\overrightarrow{\boldsymbol{\omega}_z}$ due to angular momentum drain.

We selected two different materials, one non-porous such as rock or ice ($C_1 = 1.5$, $k = 0.25$, $\mu = 0.55$) and the other porous such as sand ($C_1 = 0.55$, $k = 0.3$, $\mu = 0.41$), all constants from [20]. We do not show the spin evolution path here, but overall it is similar to Fig. 1, with a few sharp changes and mostly flat plateaus for each curve. Ceres' final spin period distribution from impacts on a non-porous or porous surface is statistically indistinguishable, 8.50 ± 0.21 hr for the non-porous case vs. 8.48 ± 0.15 hr for the porous case. However, despite the final spin period's similar distributions, these two kinds of materials do contribute differently in the mass evolution of Ceres. On average, the ejecta loss for non-porous surface is (2.69 ± 0.55) × total impactor mass, while the factor is only (0.36 ± 0.06) for porous materials. That means,

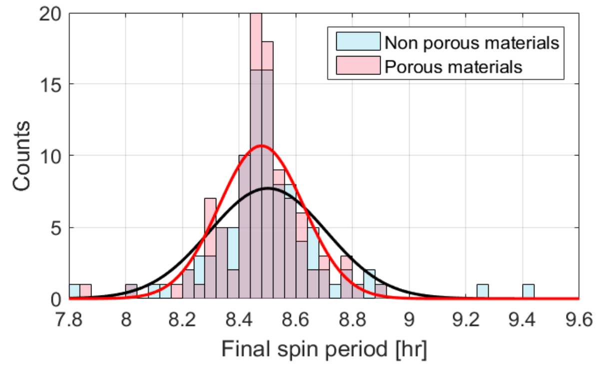

Figure 2. Histogram of final spins from two sets of simulations. Red and black curves are Gaussian references for porous and non-porous materials, respectively. Other than the range difference, these two distributions are statistically indistinguishable. See text.

Ceres must be eroding rather than accreting if the surface is non-porous, like a cemented mixture of ice and rock and salts, and so forth. In terms of whether Ceres could have been spun down, we can say that Ceres' spin is likely to have evolved somewhat from its "initial" state due to cratering, either up or down, and by a decent fraction of an hour.

Future work: Even updating [3] does not fully capture the distribution of ejecta for oblique impacts, which will further modify our results. We also plan to simulate the impacts that caused Ceres' observed cratering record more explicitly.

References: [1] McAdoo, D.C. and Burns, J.A. (1973) *Icarus*, 18, 285-293. [2] Davis, D.R. et al. (1979) In: *Asteroids*, Tuscon: University of Arizona Press. [3] Dobrovolskis, A.R. and Burns, J.A. (1984) *Icarus*, 57, 464-476. [4] Farinella, P. et al. (1992) *A&A*, 253, 604-614. [5] Harris, A.W. (1979) *Icarus*, 40, 145-153. [6] Holsapple, K.A. and Henych, T. (2016) *47th LPSC*, abs. #2897. [7] Marchi, S. et al. (2016) *Nat. Commun.*, 7, 12257. [8] Strom, R.G. et al. (2018) *Icarus*, 302, 104-108. [9] Mao, X. and McKinnon, W.B. (2018) *Icarus*, 299, 430-442. [10] Henych, T. and Pravec, P. (2013) *MNRAS*, 432, 1623-1631. [11] Park, R.S. et al. (2016) *Nature*, 537, 515-517. [12] de Elía, G.C. and Di Sisto, R.P. (2011) *A&A*, 534, A129. [13] Davison, T.M. et al. (2015) *46th LPSC*, abs. #2116. [14] Durda, D.D. et al. (1998) *Icarus*, 135, 431-440. [15] Yoshida, F. (2012) *ACM*, abs. #6063. [16] Ishida, K. et al. (1984) *Publ. Astron. Soc. Japan*, 36, 357-370. [17] Melosh, H.J. (1989) *Impact cratering: a geologic process*, New York: Oxford University Press. [18] Macke, R.J. et al. (2011) *Meteor. Planet. Sci.*, 46, 1842-1862. [19] Konopliv, A.S. et al. (2017) *Icarus*, 299, 411-429. [20] Housen, K.R. and Holsapple, K.A. (2011) *Icarus*, 211, 856-875.